NONLINEAR AEROPREDICTION METHODOLOGY FOR ROLL POSITIONS 0 AND 45 DEGREES

F. G. Moore* and R. M. McInville†
Naval Surface Warfare Center, Dahlgren Division
Dahlgren, VA 22448-5000

Abstract

The Naval Surface Warfare Center, Dahlgren Division Aeroprediction Code has been extended to the roll position of 45 deg (or fins in cross or "x" orientation). New technology developed and discussed in this paper includes: wing-body and body-wing interference factors for this roll orientation and to angles of attack of 90 deg; approximate methods to estimate wing-alone center of pressure shift at high angles of attack and 45 deg roll position; and "fin choking" at high Mach number. This new technology allows aerodynamics to be estimated with average accuracy levels of ± 10 percent on normal and axial force coefficients and ± 4 percent of body length on center of pressure. Exceptions to this are at subsonic Mach number and high angle of attack where wind tunnel sting interference effects are present, and at high Mach number and angle of attack where internal shock interactions from a forward fin onto an aft-mounted fin are present. Results are presented for several wing-body and wing-body-tail configurations at various Mach numbers and angles of attack to support this average accuracy level conclusion.

Nomenclature

AR	Aspect Ratio $= b^2/A_W$
a	Speed of Sound (ft/sec)
A_{REF}	Reference area (maximum cross-sectional area of body, if a body is present, or planform area of wing, if wing alone)(ft^2)
A_W	Planform area of wing in crossflow plane (ft^2)
b	Wing span (not including body)(ft)
C_A	Axial force coefficient

C_M	Pitching moment coefficient (based on reference area and body diameter, if body present, or mean aerodynamic chord, if wing alone)
C_N	Normal force coefficient
C_{N_B}	Normal force coefficient of body alone
$C_{N_{B(V)}}$	Negative afterbody normal-force coefficient due to canard or wing-shed vortices
$C_{N_{B(W)}}, C_{N_{B(T)}}$	Normal-force coefficient on body in presence of wing or tail
$\Delta C_{N_{B(W)}}$	Additional normal-force coefficient on body due to presence of wing
C_{N_L}	Linear component of normal-force coefficient
$C_{N_{NL}}$	Nonlinear component of normal-force coefficient
$C_{N_{T(V)}}$	Negative normal-force coefficient component on tail due to wing or canard-shed vortex
C_{N_W}	Normal force coefficient of wing alone
$C_{N_{W(B)}}$	Normal-force coefficient of wing in presence of body
$C_{N_\propto}$	Normal-force coefficient derivative
c_r	Root chord (ft)
c_t	Tip chord (ft)
C_1, C_2	Dimensionless empirical factors used in nonlinear model of $k_{W(B)}$ to approximate effects due to high AOA or control deflection
cal	Caliber(s) (one body diameter)

19961213 005

---

* Senior Aerodynamicist in Weapons Systems Department and Associate Fellow of AIAA
† Aerospace Engineer in Aeromechanics Branch of Weapons Systems Department

DTIC QUALITY INSPECTED 1

d_{ref}	Reference body diameter (ft)	Φ	Circumferential position around body where $\Phi = 0$ is leeward plane with fins in plus fin arrangement (deg)
$K_{B(W)}, K_{B(T)}$	Ratio of additional body normal-force coefficient in presence of wing or tail to that of wing or tail alone at $\delta = 0$ deg		
		∞	Free-stream conditions

$k_{B(W)}, k_{B(T)}$ — Ratio of additional body normal-force coefficient due to presence of wing or tail at a control deflection to that of wing or tail alone at $\propto = 0$ deg

$[K_{B(W)}]_{MIN}$ — Minimum value of $K_{B(W)}$ as percent of slender-body theory value

K_{B_1} — Lowest value of $[K_{B(W)}]_{MIN}$ for $\Phi = 45$ deg

$K_{W(B)}, K_{T(B)}$ — Ratio of normal-force coefficient of wing or tail in presence of body to that of wing or tail alone at $\delta = 0$ deg

$k_{W(B)}, k_{T(B)}$ — Ratio of wing or tail normal-force coefficient in presence of body due to a control deflection to that of wing or tail alone at $\propto = 0$ deg

ℓ_B — Length of body (cal or ft)

ℓ_a — Afterbody length (cal or ft)

M — Mach number = V/a

r — Radius of body (ft)

s — Wing or tail semispan plus body radius in wing-body lift methodology

V — Velocity (ft/sec)

X_{CP} — Center of pressure (in feet or calibers from some reference point that can be specified) in x direction

$\propto$ — Angle of attack (deg)

$\propto_W, \propto_T$ — Local angle of attack of wing or tail ($\propto + \delta$ in degrees)

δ — Control deflection (deg), positive leading edge up

λ — Taper ratio of a lifting surface = c_t/c_r

Introduction and Background

Many of the world's missiles fly in either the roll stabilized position of $\Phi = 0$ deg (or plus fin orientation) or $\Phi = 45$ deg (or cross fin orientation). Figure 1 illustrates these fin orientations for a cruciform missile looking from the missile nose toward the rear. As illustrated in the figure, the $\Phi = 0$ deg plane generally gives slightly more normal force and a slightly more stable configuration in pitch at a given angle of attack (AOA) than does the missile rolled to $\Phi = 45$ deg (the physics of why this occurs will be discussed in the analysis section). On the other hand, a missile in the $\Phi = 45$ deg plane is in a roll-stable position, which means less energy is required to maintain a constant roll orientation. Also, all four fins can be deflected simultaneously, giving 30 to 50 percent more normal force from control deflection than only two fins deflected in the $\Phi = 0$ deg roll position.

The latest version (1995)[1] of the Naval Surface Warfare Center Dahlgren Division (NSWCDD) Aeroprediction Code, AP95, calculates aerodynamics only in the $\Phi = 0$ deg plane. As such, aerodynamics at $\Phi = 45$ deg roll must be obtained from another aerodynamics code[2,3] or estimated from the AP95 $\Phi = 0$ deg results. It is the intent of this paper to discuss the physical phenomena that occur at the $\Phi = 0$ and 45 deg roll orientations and to summarize a semiempirical mathematical model that allows the AP95 to be extended to the $\Phi = 45$ deg plane. Details of this work can be found in Ref. 4.

The AP95 is an approximate analytical aeroprediction code primarily designed to provide preliminary estimates of aerodynamics for use in particle ballistic models, trim aerodynamic models, or structures and heat transfer models. Static aerodynamics are generally estimated with average accuracy levels of ± 10 percent and center of pressure (COP) within ± 4 percent of the body length. To obtain aerodynamics estimation accuracy levels generally desired for full six-degree-of-freedom simulations requires either a more accurate numerical code[5] or wind tunnel data or both. As such, the AP95 does not attempt to compute out-of-the-pitch-plane aerodynamics or coupling effects between the pitch and yaw planes. On the other hand, if one is interested in the $\Phi = 45$ deg plane, and control deflections are symmetric with respect to the pitch plane, then the AP95 code can be modified to allow

2

$\Phi=0°$

$\Phi=45°$

TYPICAL FORCE AND MOMENT COMPARISONS

$\Phi=0°$

$\Phi=45°$

- $(C_N)_{\Phi=0°}$ GENERALLY HIGHER THAN $(C_N)_{\Phi=45°}$ AT HIGHER α

- GENERALLY MORE STABLE IN PITCH AT $\Phi=0°$ vs $\Phi=45°$

- NATURALLY STABLE POSITION IN ROLL (LESS ENERGY TO MAINTAIN CONSTANT ROLL)

- MORE CONTROL AUTHORITY AT $\Phi=45°$ DUE TO FOUR FINS DEFLECTED vs TWO AT $\Phi=0°$

FIGURE 1. CRUCIFORM WING-BODY-TAIL MISSILE CONFIGURATION
FLYING AT ROLL OF Φ = 0 DEG AND 45 DEG

aerodynamics for the $\Phi = 45$ deg plane. These modifications will be made in an analogous process to the nonlinear semiempirical methodology of Ref. 1.

The overall approach to modify the AP95 code for nonlinear aerodynamics in the $\Phi = 45$ deg plane will thus be very similar to that for the $\Phi = 0$ deg plane.[1,6] Linearized theories or slender body theory (SBT) will be used for low AOA estimates and the data bases of Refs. 7-10 will be used to develop empirical or semiempirical corrections to account for the nonlinearities that occur in normal force and COP with increasing AOA.

Analysis

As indicated in the introduction, the goal is to develop a nonlinear semiempirical model for cruciform missiles for the $\Phi = 45$ deg plane. It is envisioned that this model will be analogous to the $\Phi = 0$ deg plane methods in AP95, except the normal force and pitching moments due to the wing alone and interference aerodynamics will have to be derived for the $\Phi = 45$ deg roll orientation.

Referring to the total normal force coefficient equation for a wing-body-tail configuration as given by Ref. 10, we have

$$C_N = C_{N_B} + \left[\left(K_{W(B)} + K_{B(W)} \right) \propto \right.$$
$$+ \left(k_{W(B)} + k_{B(W)} \right) \delta_W \left. \right] \left(C_{N\propto} \right)_W$$
$$+ \left[\left(K_{T(B)} + K_{B(T)} \right) \propto + \left(k_{T(B)} + k_{B(T)} \right) \delta_T \right] \left(C_{N\propto} \right)_T$$
$$+ C_{N_{T(V)}} + C_{N_{B(V)}} \qquad (1)$$

The $C_{N_{B(V)}}$ term of Eq. (1), which is the downwash normal force on the body due to the wing shed vortices, is neglected. This is because it is inherently included in the wind tunnel data bases, and it is believed the errors in trying to analytically estimate the term, subtract it out on one configuration, and then add it back in later on a different configuration, are as large or larger than the errors from incorporating it into the $K_{B(W)}$ term.

Equation (1) can also be rewritten as

$$C_N = C_{N_B} + C_{N_{W(B)}} + C_{N_{B(W)}}$$
$$+ C_{N_{T(B)}} + C_{N_{B(T)}} + C_{N_{T(V)}} \qquad (2A)$$

where it is understood that $C_{N_{B(T)}}$ encompasses the $C_{N_{B(V)}}$ term. For ease of implementation into an existing code designed primarily for linear aerodynamics, most of the terms in Eq. (2A) are separated into a linear and nonlinear contribution due to $\propto$ or δ. For example, the wing-body term is computed in the AP95 code as follows:

$$C_{N_{W(B)}} = \left[\left(C_{N\propto} \right)_L + \left(C_{N\propto} \right)_{NL} \right]_W$$

$$\left\{ \left[\left(K_{W(B)} \right)_{SBT} + \left(\Delta K_{W(B)} \right)_{NL} \right] \propto \right.$$

$$+ \left(C_1 \left[k_{W(B)} \right]_{SBT} + C_2 \right) \delta_W \left. \right\} \left(\frac{A_W}{A_{REF}} \right) \qquad (2B)$$

The linear or small AOA terms of Eq. (2B) are estimated by linear theory (LT) or SBT. This gives the Aeroprediction Code a good fundamental basis for its aerodynamic estimates. The nonlinear corrections due to higher AOA or control deflection are each estimated directly from component wind tunnel data bases.[7-10] Each of the other terms in Eq. (2A) is treated in a similar fashion to Eq. (2B) in the actual implementation into the Aeroprediction Code.

In the context of Eq. (2), we therefore seek the nonlinear definition of each of the terms in Eq. (2) for $\Phi = 45$ deg roll. It is expected that the body-alone term [first term of Eq. (2A)] will be independent of Φ. In reality, this is not necessarily the case for $M < 2$ and high AOA because of the asymmetric shedding of vortices. The mechanism of this shedding is not clear, but it is suspected that slight imperfections in the flow or body shape, from uniform or axisymmetric, respectively, could contribute to this phenomenon. At present, the Aeroprediction Code does not account for out-of-plane aerodynamics, and therefore the side force created by the asymmetric shedding of body vortices is not predicted. Also, in the Ref. 9 data, normal force varied by about 10 percent as a function of roll in the region of asymmetric vortex shedding. Instead of including this variation, it was averaged out.

Each of the remaining terms in Eq. (2) will be predicted in an analogous fashion to the AP95 developed for $\Phi = 0$ deg, except here the quantities will be for $\Phi = 45$ deg. As already mentioned, that approach was based on LT or SBT for small values of $\propto$ and empirical data bases (Refs. 7-10) to develop nonlinear corrections for large $\propto$. As such, it is

instructive to examine the fundamental impact of roll orientation on LT and SBT before proceeding to the nonlinear corrections, which are empirical in nature.

SBT and LT Results for Roll-Dependent Aerodynamics

References 11 and 12 were primary materials used for examining roll dependence implications from slender body and linearized theories. A somewhat detailed summary of these results is given for information purposes in Ref. 4. The summary of the key findings in Ref. 4, repeated here for convenience, are:

a) For cruciform wings alone or a wing-body combination, the total normal force is independent of roll.

b) For a planar wing-body combination at roll, the loading on the windward plane panel is greater by an amount equal to that on the leeward plane panel. This means that if one were trying to design a code for lateral aerodynamics, roll dependence of each fin planform must be considered. On the other hand, if longitudinal aerodynamics are of primary interest, the total normal force on the entire wing planform can be considered.

c) For a cruciform wing-body-tail configuration at roll, eight vortices are shed in the wing-body region, which adversely affects the tail lift. This is as opposed to four vortices at $\Phi = 0$ deg.

d) The planar theory developed for wing-tail interference can be used to approximate the loss of lift on the tails at $\Phi = 45$ deg.

e) The aerodynamics of a cruciform wing-body-tail combination with zero control deflections are independent of roll position.

These findings for roll dependence from LT or SBT are quite useful in helping plan how to develop a nonlinear aeroprediction code for $\Phi = 45$ deg. While the conclusions of LT roll dependence may not translate to the nonlinear case, we will still use the findings to help guide the nonlinear code development. In particular, the item (a) conclusion implies use of the $\Phi = 0$ deg, wing-alone data for $\Phi = 45$ deg. This is quite important because the available wing-alone data bases are all at $\Phi = 0$ deg. This means that any nonlinear wing-alone roll dependence will be included in the interference factors rather than the wing-alone solution, which is independent of Φ.

The second major result of the key SBT/LT roll dependence findings is that for cruciform missiles, we can use the same interference approaches as in the AP95, except the constants need to be changed because of a different roll angle. The combination of these two conclusions are quite important because they basically allow the direct usage of the AP95 code with different constants for the nonlinear interference terms at $\Phi = 45$ deg versus $\Phi = 0$ deg.

The third significant conclusion is that for small AOA, wing-body-tail aerodynamics are independent of roll position. This allows the usage of wing-tail interference methodology designed for planar computations for different roll orientations, so long as the proper number of vortices are considered. Again, different nonlinear corrections are expected for the $\Phi = 45$ deg versus the $\Phi = 0$ deg roll position.

Nonlinear Aerodynamics Methods

This section will describe the methods used for computing the nonlinear corrections for each of the terms in Eq. (2). These corrections, with the exception of the body alone, are all empirical in nature.

The wing- and body-alone methods for normal force coefficient prediction are quite similar to those in Ref. 1. In Ref. 1, the wing-alone normal force was estimated by a fourth order equation in AOA, with the constants chosen by the data bases of Refs. 2, 7, and 8. The body-alone normal force was predicted by linearized theory combined with a modified version of the Allen Perkins viscous crossflow theory[13] at higher AOA.

The COP of the wing at $\Phi = 0$ deg roll was estimated by LT at low AOA and assuming the COP goes to the centroid of presented area at AOA 60 deg. The body-alone COP at $\Phi = 0$ deg was estimated by a weighted average of linearized theory and viscous crossflow theory with COP shifts based on data at transonic Mach numbers. The $\Phi = 45$ deg body-alone COP is assumed to be the same as that at $\Phi = 0$ deg.

A shift in the wing-body COP at $\Phi = 45$ deg has been derived.[4] This shift is driven by the asymmetric loading that occurs on the windward to leeward plane fins as AOA is increased.

To visualize this effect, imagine a missile rolled to $\Phi = 45$ deg and increasing in AOA. As AOA increases, two things occur. First, the windward plane fins carry more and more of the load compared to the leeward plane fins. Second, the local Mach number in the windward plane is different and typically lower than the leeward plane. This has the

5

effect of shifting the wing-alone COP forward in the windward plane. Since the load and wing COPs are different on the windward and leeward plane fins, this results in a net forward shift in the COP for $\Phi = 45$ deg roll compared to the $\Phi = 0$ deg computation of Ref. (1). This shift appears to occur for all Mach numbers, is largest at moderate AOA, and goes to zero at AOA of 0 and 90 deg. At 90 deg, the windward plane fins carry almost all the load compared to the leeward plane fins, but geometrically, the fins are all aligned perpendicular to the AOA plane.

Mathematically, this geometrical shift can be approximated by:[4]

$$\left(\Delta X_{CP}\right)_{WB} = -\left[r + \left(\frac{b}{C_r + C_t}\right)\left(\frac{C_r}{2} - \frac{C_t}{3}\right)\right]$$

$$\cos(\Phi)\ \sin(2\alpha)\left(\frac{0.8\alpha}{65}\right)\ ;\ \alpha \le 65 \qquad (3A)$$

$$= -0.8\left[r + \left(\frac{b}{C_r + C_t}\right)\left(\frac{C_r}{2} - \frac{C_t}{3}\right)\right]$$

$$\cos(\Phi)\ \sin(2\alpha)\ ;\ \alpha > 65° \qquad (3B)$$

Equation (3) is added to the COP prediction at $\Phi = 0$ deg[1] for the roll orientation of 45 deg.

Wing-Body and Body-Wing Interference Due to AOA

The wing-body and body-wing interference factors were computed using a combination of the Ref. 9 data base for $0.6 \le M_\infty \le 4.6$ and the Ref. 10 data base at $M = 0.1$. Outside these Mach limits, extrapolations were made to allow the methodology to compute aerodynamics at all Mach numbers. These extrapolations were not as difficult as they may seem because normal forces and COP have basically leveled out at $M = 4.6$, and further increases in Mach number produce fairly small changes in these parameters.

The wing-body interference factor is defined as

$$K_{W(B)} = \frac{C_{N_{W(B)}}}{C_{N_w}} \qquad (4)$$

Here, $C_{N_{W(B)}}$ was measured directly in the data base of Ref. 9 by having the wing in close proximity to the body and measuring directly the load on the wing in the presence of the body. Since the normal force was measured normal to a single fin, to get the normal force on the wing in the presence of the body at $\Phi = 45$ deg from the data required the data to be multiplied by $\cos \Phi$. To reduce measurement errors, the data from all four fins were averaged. No attempt was made to correct for wind tunnel errors near zero AOA caused by flow misalignments. These errors can cause the normal force curve to be shifted as much as a degree. This means that the $C_{N_{w(B)}}$ accuracy could have some slight errors near zero AOA.

Based on the accuracy analysis of Ref. 1, fairly accurate values of $K_{W(B)}$ can be expected for all but the highest aspect ratio where the wing planform area was only about 2 percent of the body planform area in the crossflow plane. C_{N_w} of Eq. (4) was arrived at from Ref 1, which in turn used the data bases of Refs. 2, 7 and 8.

The body-wing interference factor is defined as

$$K_{B(W)} = \frac{C_{N_{B(W)}}}{C_{N_w}} \qquad (5)$$

Unfortunately, $C_{N_{B(W)}}$ was not a quantity that was measured directly in Ref. 7 but was computed from three other independent measurements of body alone, wing in conjunction with the body, and total normal force. The computation for $C_{N_{B(W)}}$ was then made by

$$C_{N_{B(W)}} = C_N - C_{N_B} - C_{N_{W(B)}} \qquad (6)$$

As shown in the Ref. 1 error analysis, this process gave potential errors that were much higher than for $C_{N_{W(B)}}$, particularly for the smaller wings ($AR \ge 1.0$) and higher Mach numbers ($M \ge 2.5$), where the $C_{N_{B(W)}}$ term decreased to the point where it was within the accuracy of the data. As a result, much more scatter in the data is expected for this term, and more engineering judgement is required in the empirical model development.

Unlike Ref. 9, Ref. 10 had a fairly large wing planform area compared to the body planform area (approximately 60 percent). Moreover, $C_{N_{B(W)}}$ was apparently measured separately. Hence, $C_{N_{B(W)}}$ could be computed based on direct measurements, as well

6

as calculated similar to Eq. (6). Also, data were obtained all the way to $\propto$ = 90 deg and at an r/s value of 0.25. As a result, more confidence is placed on the Ref. 10 body-wing interference at high AOA than the Ref. 9 data. Unfortunately, the Ref. 10 data were taken only at M_∞ = 0.1, so it is hard to extrapolate it past about M_∞ = 0.6. Fortunately, it compliments the Mach number range of the larger Ref. 9 data base quite nicely.

Figure 2 shows one example of the many figures in Ref. 4 for the nonlinear variations of $K_{W(B)}$ and $K_{B(W)}$ with AOA at M = 1.5 for aspect ratio 0.5 and at Φ = 45 deg. Other Mach number and aspect ratio results are given in Ref. 4. It is clear in examining Fig. 2, and the other figures in Ref. 4, that inclusion of the nonlinearities in the interference factors is essential in accurately developing a semiempirical nonlinear aeroprediction code. Reference 4 does this similarly to Ref. 1, where a mathematical model is developed based on SBT/LT plus deviation of SBT/LT based on data. That is,

$$K_{W(B)} = \left[K_{W(B)}\right]_{SBT} + \Delta K_{W(B)} \ (\propto, \ M, \ AR, \ \lambda)$$

$$K_{B(W)} = \left[K_{B(W)}\right]_{SBT}^{LT} + \Delta K_{B(W)} \ (\propto, \ M, \ AR, \ \lambda) \quad (7)$$

The functions $\Delta K_{W(B)}$ and $\Delta K_{B(W)}$ are defined by 11 tables in Ref. 4.

Two of the key issues associated with defining the functions $\Delta K_{W(B)}$ and $\Delta K_{B(W)}$ are the variations with r/s and internal shocks. Most of the data available[9] is for r/s of 0.5 with only one set of lifting surfaces present. This means any nonlinearities associated with r/s and internal shocks from forward to rearward lifting surfaces have to be modeled separately or not included. The most critical of these issues appeared to be the minimum value of $K_{B(W)}$ at high AOA.

Figure 3 represents the treatment of $[K_{B(W)}]_{MIN}$ for both the Φ = 0 and Φ = 45 deg roll positions. This figure was derived based on the Ref. 9 and 10 data bases for r/s = 0.5 and numerical experiments for other r/s cases. Referring to Fig. 3, note that for r/s $\leq$ 0.2, Φ = 0, there is a difference in the minimum value of $K_{B(W)}$ depending on whether there is an afterbody present or not; whereas for r/s $\geq$ 0.5, there did not appear to be. It should be remembered that $[K_{B(W)}]_{MIN}$ is given as a fraction of SBT in Fig. 3. Thus, a value of 1.0 at r/s = 0.2 in Fig. 3 gives a value of $[K_{B(W)}]_{MIN}$ of 0.27; whereas, a value of 0.5 for r/s = 0.5 gives a value of $[K_{B(W)}]_{MIN}$ of 0.4. Also worthy of note is the fact that $[K_{B(W)}]_{MIN}$ appeared to approach zero at high Mach number. More data or computational fluid dynamics are needed to more precisely define Fig. 3.

FIGURE 2. WING-BODY AND BODY-WING INTERFERENCE FACTORS AS A FUNCTION OF AOA (M_∞ = 1.5, r/s = 0.5)
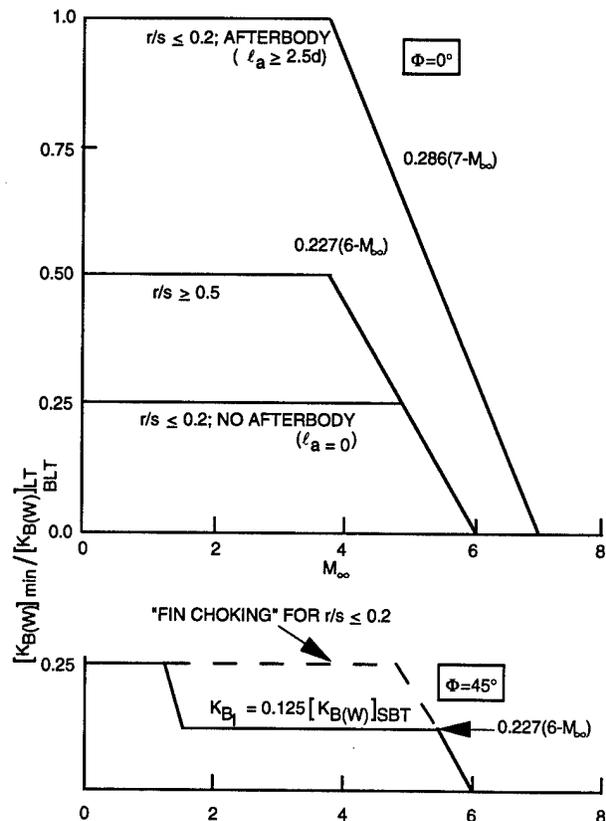
FIGURE 3. MINIMUM VALUE OF BODY-WING INTERFERENCE FACTOR AT HIGH AOA

7

Of equal importance in Fig. 3 is the lower curve for $\Phi = 45$ deg. Note that $[K_{B(W)}]_{MIN}$ is one-half to one-quarter of that for $\Phi = 0$ deg. This appears to be the main reason many missiles have lower normal forces flying at $\Phi = 45$ deg than at $\Phi = 0$ deg, particularly if r/s is fairly high (0.4 or greater). Note also the fact that "fin choking" is given a separate label for low r/s and $\Phi = 45$ deg.

"Fin choking" is a phenomenon similar to that which occurs when an inlet becomes unstarted or a wind tunnel achieves its maximum rate of flow (an increase in power produces no more mass flow through the inlet). As the body increases in AOA with the fins oriented in the "x" or cross orientation, the flow between the fins will eventually "choke" at some AOA and at moderate to large supersonic Mach numbers. When this happens, a strong shock is formed just in front of the fin,[18,19] producing a high pressure region on the fins and body. This high pressure region is shifted forward from where it would be if supersonic flow occurred through the fins. While the absolute value of pressure on the body is higher than for the unchoked flow, it occurs over a much smaller region and hence gives only slightly higher body-wing interference lift. Modified Newtonian Theory was used in Ref. 4 to define the region where "fin choking" occurred. It was seen that "fin choking" appears to occur on wing-dominated (small r/s) configurations at $\Phi = 45$ deg roll, but not on body-dominated configurations (large r/s). A fairly thorough discussion of other internal shock interactions was also given in Ref. 4. Suffice it to say that additional work is still needed before internal shock interactions can be completely modeled with a semiempirical code.

Wing-Body and Body-Wing Interference Due to Control Deflection

The same general approach, with slight modifications, to the nonlinear model of Ref. 1 for $\Phi = 0$ deg roll is used for the $\Phi = 45$ deg roll position. In the Ref. 1 method, $k_{W(B)}$ and $k_{B(W)}$ were approximated by

$$k_{W(B)} = C_1(M) \left[k_{W(B)}\right]_{SBT} + C_2(|\propto_w|, M) \quad (8)$$

$$k_{B(W)} = \left[k_{B(W)}\right]_{SBT} \quad (9)$$

The parameters C_1 and C_2 were derived based on numerical experiments of the AP95 compared to data. This was because many of the fins in the Ref. 9 data base were too small to allow accurate estimates of $k_{W(B)}$ as a function of parameters of interest. As a result, total missile load data were used and empirical values of C_1 and C_2 estimated as a function of

combined local AOA of the wing $|\propto + \delta|$, and Mach number. The tables of C_1 and C_2 for $\Phi = 45$ deg are given in Ref. 4.

In examining the constants and model of Ref. 4, several physical phenomena occur that are modeled in a semiempirical sense by Eqs. (8) and (9). These phenomena are qualitatively shown in Fig. 4. At low Mach number, Fig. 4 indicates the SBT gives a low value of $k_{W(B)}$ for small values of $\propto_w$. At a value of $\propto_w$ of about 25 deg, the controls lose effectiveness as a result of a combination of stall and blow-by effects due to the separation between the wing and body. At an $\propto_w$ of about 55 deg, the controls have lost all effectiveness. At Mach numbers greater than about 4, the controls initially generate less effectiveness than is generated by SBT for values of $\propto_w$ up to about 20 or 25 deg. The controls then become more effective because of nonlinear compressibility effects. On the other hand, at an $\propto_w$ of around 45 to 50 deg, the controls once again begin to lose effectiveness, presumably because of shock interactions and blow-by effects. For Mach numbers in between subsonic and high supersonic, $k_{W(B)}$ has behavior in between the two extremes illustrated in Fig. 4.
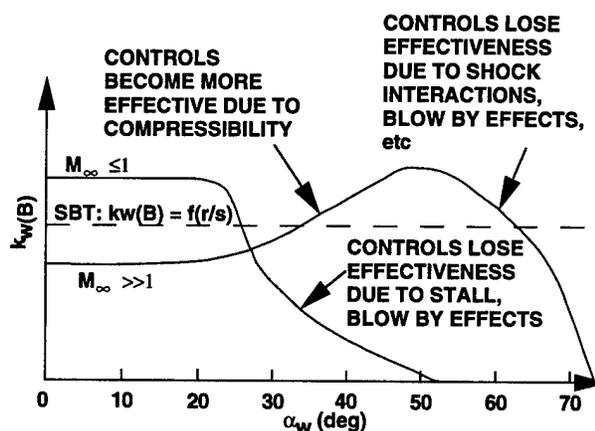
FIGURE 4. QUALITATIVE TREND OF WING-BODY INTERFERENCE DUE TO CONTROL DEFLECTION AS FUNCTION OF $(M_\infty, \propto_w)$

In comparing the nonlinear control deflection models for $\Phi = 0$ and 45 deg roll in Ref. 4, a lot of similarity is seen. The constants for $\Phi = 45$ deg are slightly different than those for $\Phi = 0$ deg and the values of $\propto_w$ where the nonlinearities begin are somewhat different. However, by and large, Eq. (8) holds for both the $\Phi = 0$ and 45 deg roll cases. It should be pointed out that in Ref. 1, mostly linear variations of $k_{W(B)}$ with $\propto_w$ were used. However, these have been improved upon for the $\Phi = 45$ deg case with cubic fits of control deflection data. As such, all nonlinear effects are included in the variations of $k_{W(B)}$ as a function of Mach number and $|\propto + \delta|$. It

8

should also be noted that $k_{W(B)}$ and $k_{B(W)}$ are multiplied by 1.414 to indicate that all four fins are assumed to be deflected by an equal amount in the $\Phi = 45$ deg roll position.

Reference 4 also derived new semiempirical models for wing-tail interference. This is the subject of another paper and is thus not discussed here. However, the comparisons with data in the <u>Results and Discussion</u> section have the new wing-tail interference model included when the configuration has two sets of lifting surfaces present.

<u>Results and Discussion</u>

The new nonlinear aeroprediction methodology for the $\Phi = 45$ deg roll position has been validated against many configurations within and outside the data bases upon which the methodology was developed. Reference 4 gives results for seven wing- or tail-body cases and five wing- or canard-body-tail cases. Three cases are chosen here to illustrate the accuracy of the new methodology as well as illustrate remaining problems in the state-of-the-art in both experimental testing and semiempirical code development. Two of these cases are given in Ref. 4 in more detail, and the third case has not been shown previously for the $\Phi = 45$ deg roll aerodynamics.

The first of these cases is from Ref. 16 and is referred to as the air-slew-demonstrator-vehicle. Data were available at both $\Phi = 0$ and 45 deg roll at $M = 0.6$ to 1.3 and to AOA 90 deg. Figure 5 shows the configuration schematically and the normal force coefficient results for $M = 0.6$, 0.9, and 1.3. This case was chosen for several reasons. First, it illustrates the accuracy of the code at both $\Phi = 0$ and 45 deg at moderate subsonic Mach numbers to AOA 90 deg. Secondly, it illustrates a problem encountered in validating the code at subsonic and transonic Mach numbers based on wind tunnel data. This problem is wind tunnel model sting interference.

Reviewing some of the wind tunnel model support interference literature (Refs. 17-20), several conclusions were reached. These were that: a) For low Mach number, the problem of estimating interference effects of a strut or sting mount on the model aerodynamics at high AOA are not known precisely—this is still true today. b) The preferable mount between a sting and a strut at high AOA is the sting. c) The sting tends to give positive interference (C_N too high) and the strut negative interference (C_N too low).

The affected region seems to be in the AOA range 30-80 deg. Sting C_N values can be high as much as 10-15 percent, and strut C_N values for struts mounted in the mid-body region can be low by as much as

25-30 percent. For these reasons, the Improved Aeroprediction Code 1995 (IAP95) methodology is intentionally designed to underpredict normal force on configurations at subsonic Mach numbers at high AOA, where test data are from a sting mount and therefore it is also expected the predictions will be higher than those from a strut-mounted model. The under/overprediction problem on C_N at high $\propto$ appears to go away at Mach numbers slightly greater than one. This is suspected to be due to the reduction in the upstream influence of the sting on the body and the reduction of the wake effect on the body (strut mount).

Since the Fig. 5 configuration was mounted in the tunnel with a strut, this is suspected to be the major reason for the overprediction of the IAP95 methodology compared to data at $M = 0.6$, 0.9 and AOA > 50 deg. While COP predictions are not shown, results are within the ± 4 percent of body length goal at all AOA and Mach numbers. This implies any loss of normal force due to the strut is distributed all along the body. Also, if one excludes the AOA > 50 deg comparison at $M = 0.6$ and 0.9 where wind tunnel measurement errors are in question, the IAP95 is well within the ± 10 percent accuracy goal on normal force as well.

The last two configurations considered in the validation process utilize all the new nonlinear methodology developed for both the $\Phi = 0$ and 45 deg roll orientations. The first of these is a version of the SEASPARROW missile as shown in Fig. 6, with wind tunnel results taken from Ref. 21. This configuration has fairly large wings and tails, with the wings used as the control. Data were taken at Mach numbers of 1.5, 2.0, 2.35, 2.87, 3.95 and 4.63. Figs. 6B, 6C, and 6D give comparisons of the IAP95 with the data at $M = 1.5$, 2.87, and 4.63 respectively. Results are shown for control deflections of 10 deg for $M = 1.5$ and 20 deg for $M = 2.87$ and 4.63. Also, all results for both the $\Phi = 0$ and 45 deg roll positions are shown. Several comments are in order with respect to the overall comparisons. First of all, the IAP95 model achieves its goal of predicting average accuracy of C_A, C_N of ± 10 percent and X_{CP} of ± 4 percent ℓ_B on this configuration at both the $\Phi = 0$ and 45 deg roll positions. Secondly, C_N is predicted equally well at $\Phi = 0$ and 45 deg. However, C_M is predicted better at $\Phi = 45$ deg than at $\Phi = 0$ deg due to the COP shift discussed earlier. No such shift has been applied at $\Phi = 0$ deg. Apparently one is needed, but it is not clear what the physical justification is. As seen in the pitching moment predictions for the $\Phi = 0$ deg roll orientation, the IAP95 in general is slightly too stable. The third point is that C_A prediction is slightly better for the $\Phi = 0$ deg roll orientation than the $\Phi = 45$ deg position. Apparently, the factor of 1.414 applied to
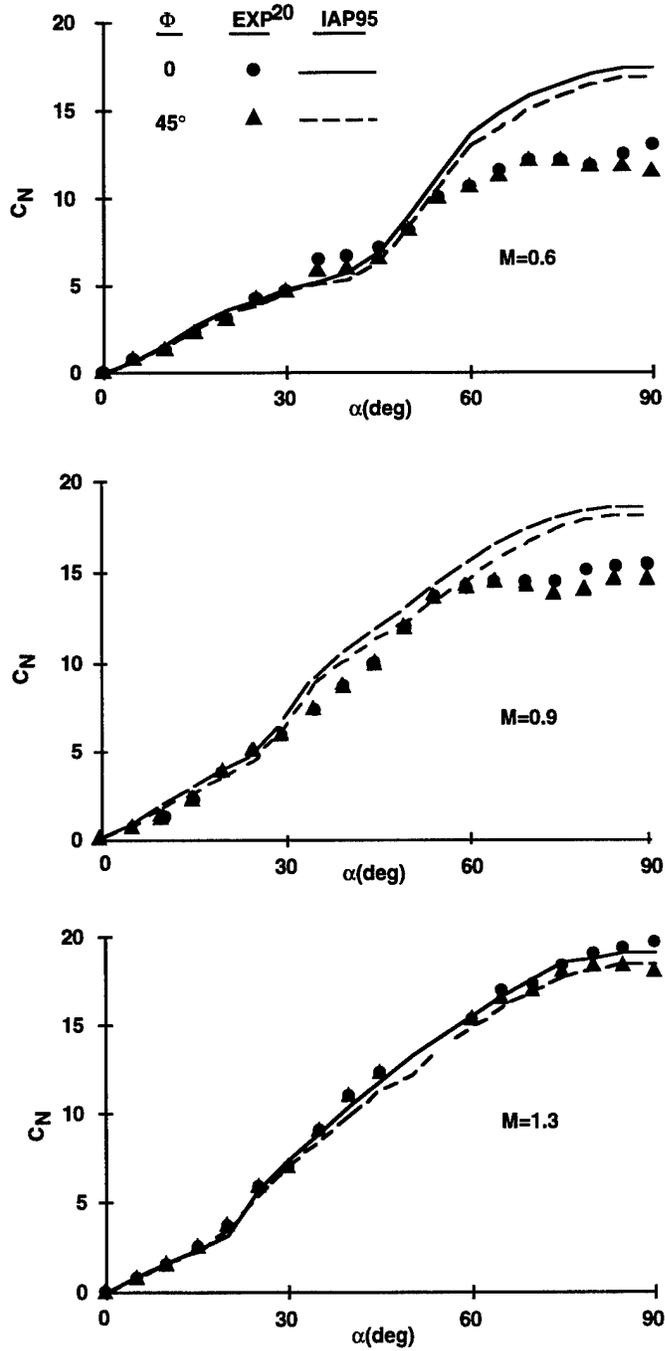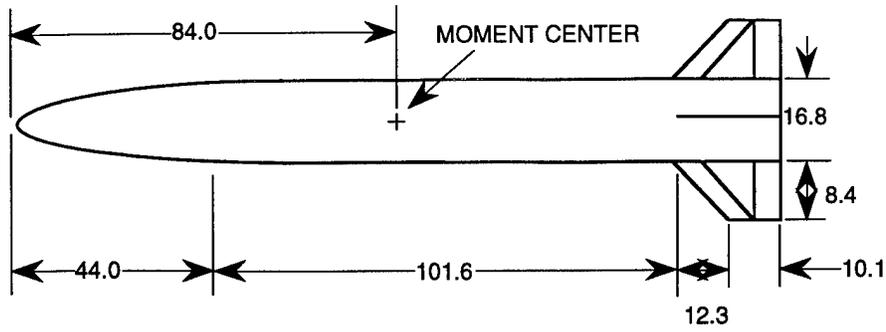
FIGURE 5. NORMAL FORCE COMPARISONS OF THEORY AND EXPERIMENT

the fins for the control deflection component of axial force is quite adequate at low AOA at all Mach numbers, as seen in the figures. However, at high AOA, this factor appears to be too high at the lower supersonic Mach numbers and too low at the higher supersonic Mach numbers. It is suspected that at the lower supersonic Mach numbers, only the fins in the windward plane should have the full factor of $\sqrt{2}$, whereas those in the leeward plane should have a lower factor. For high supersonic conditions, it is suspected the bow shock and internal shock interactions actually add to the factor of $\sqrt{2}$. An empirical model for the control deflection component of C_A to account for this physics would improve the C_A comparison, but time did not permit this effort.
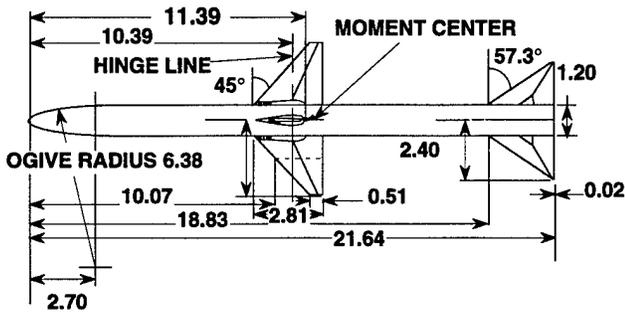
FIGURE 6A. AIR-TO-AIR MISSILE
CONFIGURATION USED IN VALIDATION
(FROM REF. 21)

The final point to be made is concerning the high Mach number, high AOA conditions in Fig. 6. Notice that the pitching moment suddenly loses stability above AOA of 30 deg and $\Phi = 0$ deg roll at $M = 4.63$. The normal force also decreases somewhat as well. It is believed this is due to internal shock waves from the bow shock and wing shock intersecting the tail, causing a loss of tail lift and a sudden decrease in stability. No accounting of these internal shocks from a forward mounted fin to an aft mounted fin is made in the IAP95. It is also interesting to note that above AOA 70 deg, while the results are not shown, the IAP95 predictions for pitching moment agree quite well with the data. Apparently the internal shock interactions are important between AOA of about 30 to 60 deg.

The last configuration chosen for validation of the new methodology against wind tunnel results is shown in Fig. 7A. The data as well as DATCOM[3] results are taken from Ref. 22. The control is from the canards. The configuration is over 22 cal in length with aspect ratio tails of 0.9 and canards 1.57. Data were taken for Mach number of 0.2 but to AOA of 50 deg with control deflections of 0 and ±20 deg. The ±20 deg control deflection cases are illustrated in Fig. 7B. Both the IAP95 and Missile DATCOM results from Ref. 22 are shown along with the data for
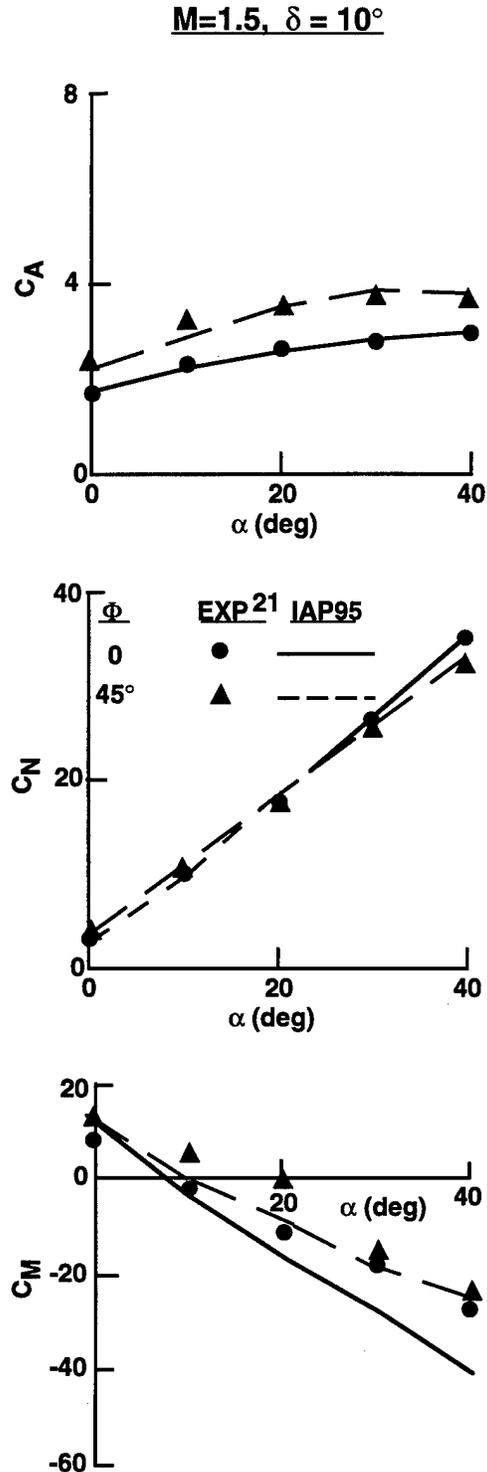
FIGURE 6B. AXIAL, NORMAL, AND
PITCHING MOMENT COEFFICIENT
COMPARISON OF THEORY AND
EXPERIMENT

M=2.87. δ = 20°

M=4.63. δ = 20°
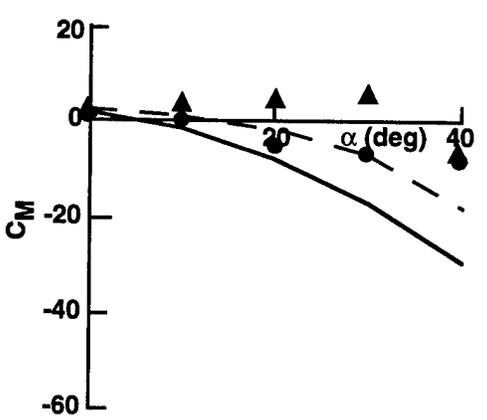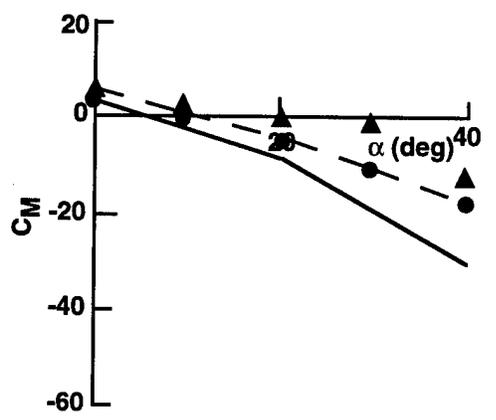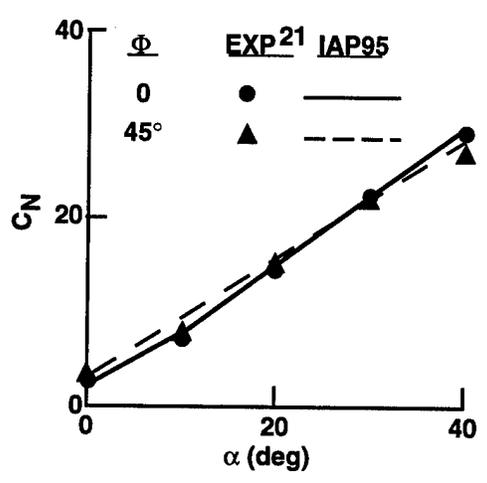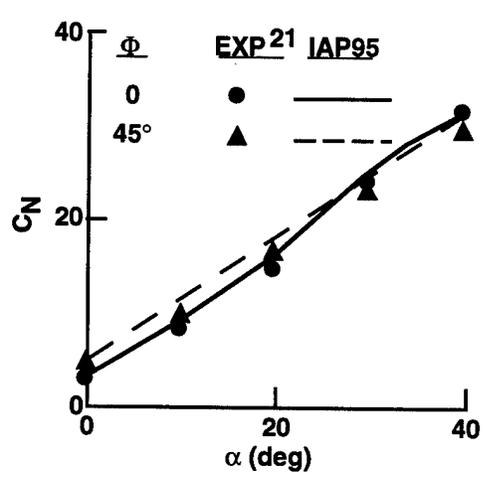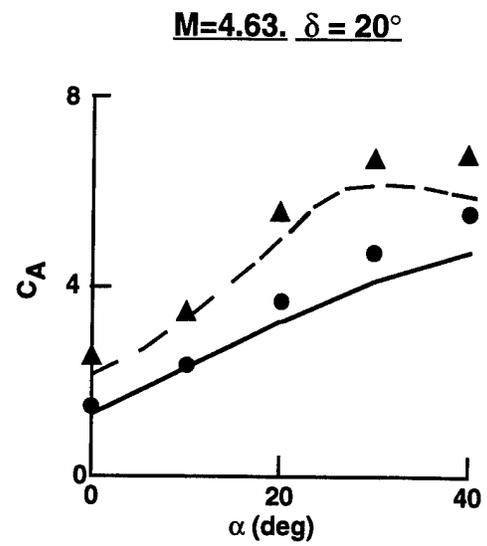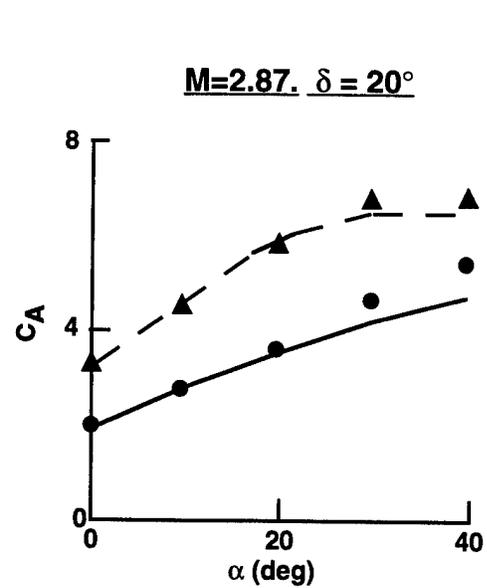
FIGURE 6C. AXIAL, NORMAL, AND
PITCHING MOMENT COEFFICIENT
COMPARISON OF THEORY AND
EXPERIMENT

FIGURE 6D. AXIAL, NORMAL, AND
PITCHING MOMENT COEFFICIENT
COMPARISON OF THEORY AND
EXPERIMENT

12

Φ = 45 deg roll only. In general, the IAP95 gives very good comparisons with data and appears to exhibit most of the nonlinearities of the data. The δ = +20 deg IAP95 predictions agree with the data slightly better than δ = -20 deg. Missile DATCOM results also give reasonably good agreement with data. Reference 1 compared the AP95, Missile DATCOM and data for this same case at Φ = 0 deg roll. The AP95 results were about as good at Φ = 0 as Φ = 45. However, the Missile DATCOM gave better results compared to data at Φ = 45 deg versus Φ = 0 deg. It is not known whether this statement holds true in general, however.
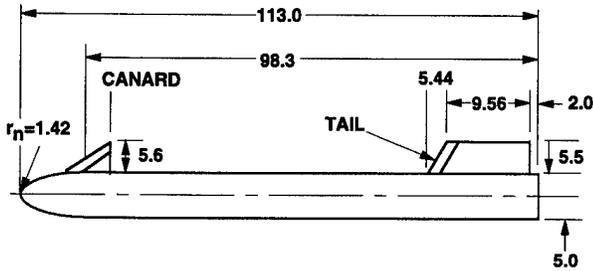
FIGURE 7A. CANARD CONTROLLED MISSILE CONFIGURATION (ALL DIMENSIONS IN INCHES, FULL SCALE)

Summary, Conclusions and Recommendations

New technology has been developed to allow engineering estimates of aerodynamics of most tactical weapon concepts for the Φ = 45 deg roll position (fins oriented in "x" or cross-fin arrangement). New technology developed for the Φ = 45 deg roll position and discussed in this paper includes:

a) Nonlinear wing-body and body-wing interference factor methodology due to AOA and control deflection.

b) An approximate method to estimate wing-alone shift in COP at Φ = 45 deg and high AOA.

c) An approximate method to account for "fin choking" at high Mach number and AOA

This new technology, along with the Φ = 0 methodology of Ref. 1, now allows trim aerodynamics to be computed in the two roll-stabilized planes that most of the world's missiles fly. The data bases upon which the methodology was based were limited in Mach number to 4.5 and AOA of 40 deg. However, engineering judgement and other data were used to allow calculations to be performed to AOA 90 deg, Mach numbers up to 20, for axisymmetric solid rocket weapons with up to two sets of lifting surfaces.

Based on the new methodology and computations to date, the following conclusions are made.

a) The two primary reasons missile normal forces are lower at Φ = 45 deg than at Φ = 0 deg are that the minimum value of body carryover lift at high AOA is lower for Φ = 45 than Φ = 0. The larger the value of r/s, the more difference between these minimum values. If the configuration has two sets of lifting surfaces, the wing-tail interference is higher for AOA > 20 deg for the Φ = 45 deg plane than for the Φ = 0 deg plane, also contributing to a lower normal force for Φ = 45 deg and a less stable configuration.

b) At high AOA: $K_{W(B)}$ approaches 1.0 for most Mach numbers; $K_{B(W)}$ approaches some minimum value that is a function of r/s and Mach number; $k_{W(B)}$ and $k_{B(W)}$ are nonlinear in total local AOA on the wing and are functions of Mach number and total AOA on the wing.

c) "Fin choking" appears to be more of a problem on larger fin (small r/s) configurations at Φ = 45 deg than on smaller fin cases (large r/s).

d) For Mach numbers less than one and AOA > 30 deg, it is not clear what the correct values of experimental normal force are for a given configuration, based on wind tunnel results available in the literature.

e) Internal shock interactions between forward-mounted and aft-mounted fins become increasingly important as both AOA and Mach number increase. The current methodology does not account for these effects.

f) In general, ±10 percent average accuracy has been maintained for both normal and axial force coefficients and ±4 percent of body length for COP in the Φ = 45 deg roll position. Exceptions to this are at subsonic Mach number and high AOA where data accuracy is in question, and at high Mach number and high AOA for configurations that have two sets of lifting surfaces, where internal shock interactions may be a problem.

g) The current overall approach of using linear theory, slender body theory, or second order theory for low AOA aerodynamics, and estimating the nonlinear aerodynamic terms

13
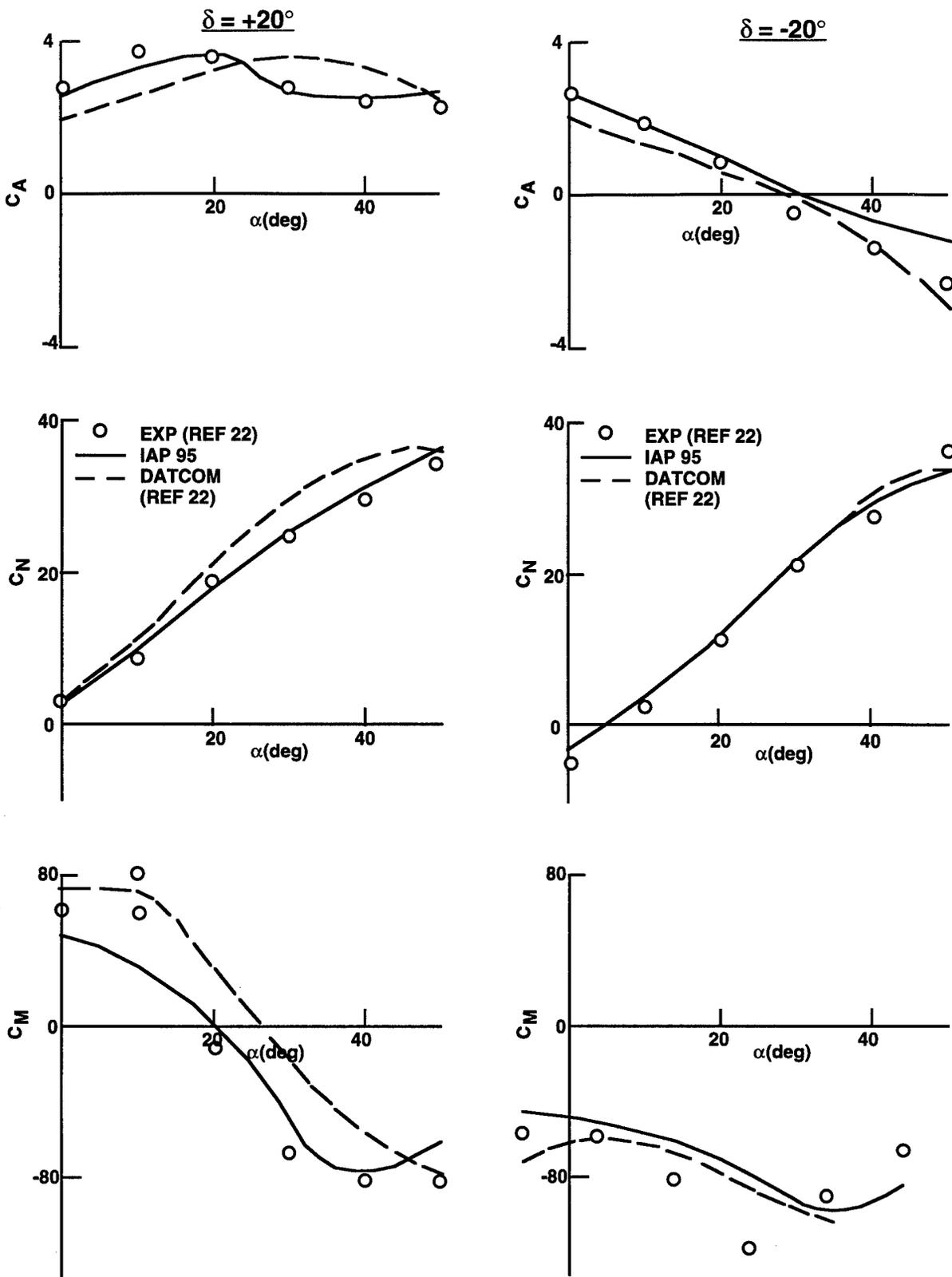
FIGURE 7B. AXIAL, NORMAL, AND PITCHING MOMENT COEFFICIENT
COMPARISONS OF THEORY AND EXPERIMENT
(M = 0.2, Φ = 45 DEG)

individually and directly from wind tunnel data bases, appears to be the key to the above-mentioned average accuracy levels.

Based on this and previous research (Refs. 1, 6), the following recommendations are made for additional work:

a) Additional wind tunnel measurements or computational fluid dynamics cases need to be made to help define nonlinearities of the interference effects as a function of r/s.

b) A method is needed to accurately correct wind tunnel data at subsonic Mach number and high AOA for sting or strut mounting effects.

c) An engineering method is needed to estimate internal shock interaction effects for high AOA and Mach number.

d) Any future wind tunnel test for measuring component aerodynamics should be done with lifting surfaces large enough to separate out body and wing lift accurately, with wings mounted in the middle of the body and, preferably, with simultaneous measurements of body forces in conjunction with the wing and wing forces in conjunction with the body. This would allow more accurate determination of the interference terms directly, without subtraction of two large numbers to obtain a small term.

Acknowledgment

References

1. Moore, F. G., McInville, R. M., and Hymer, J. C., "The 1995 Version of the NSWC Aeroprediction Code: Part I - Summary of New Theoretical Methodology," NSWCDD/TR-94/379, Feb. 1995.

2. Nielsen, J. N., Hemsch, M. J., and Smith, C. A., "A Preliminary Method for Calculating the Aerodynamic Characteristics of Cruciform Missiles to High Angles of Attack Including Effects of Roll Angle and Control Deflections," ONR-CR215-226-4F, 800 N. Qunicy St., Arlington, VA 22217.

3. Williams, J. E., and Vukelich, S. R., "USAF Stability and Control DATCOM," AFFDL-TR-75-45, Wright Patterson Air Force Base, Dayton, OH.

4. Moore, F. G., and McInville, R. M., "Extension of the NSWCDD Aeroprediction Code to the Roll Position of 45 Degrees," NSWCDD/TR-95/160, Dec. 1995.

5. Wardlaw, A. B., and Davis, S., "A Second-Order Gudonov Method for Supersonic Tactical Missiles," NSWC TR-86-506, 1986, NSWC, Dahlgren, VA.

6. Moore, F. G., Hymer, T., and Devan, L., "New Methods for Predicting Nonlinear Lift, Center of Pressure, and Pitching Moment on Missile Configurations," NSWCDD/TR-92/217, Jul. 1992, Dahlgren, VA.

7. Stallings, R. L., Jr., and Lamb, Milton, "Wing-Alone Aerodynamic Characteristics for High Angles of Attack at Supersonic Speeds," NASA Technical Paper 1889, Jul. 1981.

8. Baker, W. B., Jr., "Static Aerodynamic Characteristics of a Series of Generalized Slender Bodies With and Without Fins at Mach Numbers from 0.6 to 3.0 and Angles of Attack from 0 to 180°," AEDC-TR-75-124, Vol. I and II, May 1976, Tullahoma, TN.

9. NASA Langley Research Center Tri-Service Missile Data Base, Transmitted from NASA/LRC Jerry M. Allen to NAVSWC on 5 Nov. 1991 (formal documentation in process)

10. Meyer, J., "Effects of the Roll Angle on Cruciform Wing-Body Configurations at High Incidences," Journal of Spacecraft and Rockets, Vol. 31, No. 1, Jan.-Feb. 1994, pp. 113-122.

11. Ashley, Holt, Landahl, and Martin, *Aerodynamics of Wings and Bodies*, Addison - Wesley Publishing Company, Inc., Reading, MA, Copyright 1965.

12. Nielsen, J. N., *Missile Aerodynamics*, NEAR, Inc., Mountain View, CA, 1988.

13. Allen, J. H., and Perkins, E. W., "Characteristics of Flow Over Inclined Bodies of Revolution," NACA RM A 50L07, Mar. 1951.

14. Stallings, R. L., Jr., Lamb, M., Watson, C. B., "Effect of Reynolds Number on Stability Characteristics of a Cruciform Wing-Body at Supersonic Speeds," NASA TP 1683, Jul. 1980.

15. Agnone, A. M., Zakkay, V., Tory, E., and Stallings, R., "Aerodynamics of Slender Finned Bodies at Large Angles of Attack," AIAA Paper 77-0666, 10th Fluid and Plasma Dynamics Conference, Albuquerque, NM, Jun. 1977.

16. Whoric, J. M., and Washington, E. S., "Aerodynamic Characteristics of the Air Slew Demonstrator Models at Mach Numbers 0.6 to 1.3," AEDC TR-76-92, Aug. 1976.

17. Dietz, Jr., and Altstatt, M. C., "Experimental Investigation of Support Interference on an Ogive Cylinder at High Incidence," Journal of Spacecraft and Rockets paper Vol. 16, No. 2, Mar.-Apr. 1979, pp. 67-68.

18. Canning, T. N., and Nielsen, J. N., "Experimental Study of the Interference of Supports on the Aerodynamic Loads on an Ogive Cylinder at High Angles of Attack," AIAA paper 81-0007, 19th Aerospace Sciences Meeting, Jan. 12-15, St. Louis, MO.

19. Nelson, R. C., and Mouch, T. N., "Cylinder/Splitter-Plate Data Illustrating High $\propto$ Support Interference," Journal of Spacecraft and Rockets Note, Vol. 16, No. 2, Mar.-Apr. 1979, pp. 126-127.

20. Ericsson, L. E., and Reding, J. P., Review of Support Interference in Dynamic Tests, AIAA Journal, Dec. 1983, pp. 1652-1662.

21. Monta, W. J., "Supersonic Aerodynamic Characteristics of a Sparrow III Type Missile Model with Wing Controls and Comparison with Existing Tail Control Results," NASA TP 1078, Nov. 1977.

22. Smith, E. H., Hebbar, S. K., and Platzer, M., "Aerodynamic Characteristics of a Canard-Controlled Missile at High Angles of Attack," AIAA paper No. 93-0763, presented at 31st Aerospace Sciences meeting, Reno, NV, 11-14 Jan. 1993.

PLEASE CHECK THE APPROPRIATE BLOCK BELOW: M97-03-2025

☐ _____A_____ copies are being forwarded. Indicate whether Statement A, B, C, D, E, F, or X applies.

☒ DISTRIBUTION STATEMENT A:
APPROVED FOR PUBLIC RELEASE: DISTRIBUTION IS UNLIMITED

☐ DISTRIBUTION STATEMENT B:
DISTRIBUTION AUTHORIZED TO U.S. GOVERNMENT AGENCIES ONLY; (Indicate Reason and Date). OTHER REQUESTS FOR THIS DOCUMENT SHALL BE REFERRED TO (Indicate Controlling DoD Office).

☐ DISTRIBUTION STATEMENT C:
DISTRIBUTION AUTHORIZED TO U.S GOVERNMENT AGENCIES AND THEIR CONTRACTORS; (Indicate Reason and Date). OTHER REQUESTS FOR THIS DOCUMENT SHALL BE REFERRED TO (Indicate Controlling DoD Office).

☐ DISTRIBUTION STATEMENT D:
DISTRIBUTION AUTHORIZED TO DOD AND U.S. DOD CONTRACTORS ONLY; (Indicate Reason and Date). OTHER REQUESTS SHALL BE REFERRED TO (Indicate Controlling DoD Office).

☐ DISTRIBUTION STATEMENT E:
DISTRIBUTION AUTHORIZED TO DOD COMPONENTS ONLY; (Indicate Reason and Date). OTHER REQUESTS SHALL BE REFERRED TO (Indicate Controlling DoD Office).

☐ DISTRIBUTION STATEMENT F:
FURTHER DISSEMINATION ONLY AS DIRECTED BY (Indicate Controlling DoD Office and Date) or HIGHER DOD AUTHORITY.

☐ DISTRIBUTION STATEMENT X:
DISTRIBUTION AUTHORIZED TO U.S. GOVERNMENT AGENCIES AND PRIVATE INDIVIDUALS OR ENTERPRISES ELIGIBLE TO OBTAIN EXPORT-CONTROLLED TECHNICAL DATA IN ACCORDANCE WITH DOD DIRECTIVE 5230.25, WITHHOLDING OF UNCLASSIFIED TECHNICAL DATA FROM PUBLIC DISCLOSURE, 6 Nov 1984 (Indicate date of determination). CONTROLLING DOD OFFICE IS (Indicate Controlling DoD Office).

☐ This document was previously forwarded to DTIC on _____ (date) and the AD number is _____.

☐ In accordance with the provisions of DoD instructions, the document requested is not supplied because:

☐ It is TOP SECRET.

☐ It is excepted in accordance with DoD instructions pertaining to communications and electronic intelligence.

☐ It is a registered publication.

☐ It is a contract or grant proposal, or an order.

☐ It will be published t a later date. (Enter approximate date, if known.)

☐ Other. (Give Reason.)

Frank Moore
Print or Typed Name

Frank Moore
Authorized Signature Date

540-653-8831
Telephone Number

#63 Nonlinear Aeroprediction methodology for Roll Positions 0 and 45 Degrees 6B